

Novel Autonomous Self-aligning Wireless Power Transfer for Improving Misalignment

Milad Behnamfar, Mohd Tariq and Arif I. Sarwat

Department of Electrical and Computer Engineering, Florida International University, Miami, Florida, USA

ARTICLE INFO

Keywords:
Stationary Charging
Misalignment Performance
Coupling Coefficient
Wireless Power Transfer
Inductive Power Transfer
Self-aligning mechanism
Robot
Magnetic Field Sensor
Inductive Coil

ABSTRACT

A novel autonomous self-aligning wireless power transfer for solving misalignment issues in stationary charging of electric vehicles is proposed. Misalignment between transmitter and receiver is the most serious obstacle in the charging process of stationary charging of electric vehicles, which hampered this technology to be commercialized widespread. To improve the misalignment performance, a moveable transmitter is proposed, in which the transmitter pad is mounted on a robot. The robot is equipped with a magnetic field sensor, which the sensor is installed in the center of the circular transmitter pad. By using the proposed algorithm, the transmitter's coil mounted on the robot follows the receiver, based on measuring the magnetic field. In this case, by having misalignment, the robot moves the transmitter pad to remove misalignment and create alignment. For validating the proposed self-aligning mechanism, an experiment test has been done, and the experimental results show the effectiveness of the proposed mechanism in aligning the transmitter pad with the receiver pad. The design process and implementation of the robot by considering the transmitter's coil weight, and the required torque to move the transmitter's coil are discussed.

1. Introduction

Electric vehicles have gained more popularity in the past few years as it resolves the detrimental effects of fuel-cell vehicles on the environment. Many car manufacturers turn their focus on manufacturing electric vehicles and electric vehicles have been commercialized in widespread. However, plug-in charging of electric vehicles suffers from range anxiety and a long duration time of charging. In addition, Leakage from fractured old cables, especially in cold regions, might create extra hazards for the user. For the plug-in charging, users have to endure the snow, rain, and wind to charge their vehicles. Moreover, Users may forget to plug in and eventually run out of battery power the next time when they want to use the electric vehicle [1].

Wireless power transfer for charging electric vehicles was proposed to address the drawback of plug-in charging. Wireless charging is convenient, and without human interference, the charging process can automatically start when the receiver installed under the chassis of the electric vehicle is aligned with the transmitter's pad underground. Wireless power transfer based on energy transfer is classified as Inductive power transfer (IPT) and Capacitive power transfer (CPT), utilizing the magnetic field and electric field respectively to transfer power[2]. The CPT system offers two benefits over the IPT system. First and foremost, the CPT system is insensitive to nearby metal objects, and secondly, due to using metal plates to transfer power, the CPT system is cost-efficient. However, the CPT system efficiency is much lower than the IPT system, and it has safety issues due to the electric field emission to the environment around the coupler [3]. Because of the mentioned reasons, the IPT system is widely used for wireless charging of electric vehicles.

The wireless power transfer for charging electric vehicles is classified into two groups: stationary and dynamic charging. In stationary charging, to begin the charging process

only required the vehicle to be parked on the transmitter's pad installed beneath the ground. Dynamic charging enables electric vehicles to be charged while driving, which increases the driving range and decreases the battery's weight and cost [4]. In both technologies, misalignment is the biggest hurdle to effectively charging electric vehicles. In dynamic charging, the misalignment gives rise to coupling variation between the receiver and transmitter's coil, which lead to power pulsation at the battery side. Power pulsation is harmful to the battery's lifetime. Misalignment for the stationary charging scenario is even worse, which in most cases, ceases the power transfer from the primary side to the secondary side.

Depending on standards and recommendations, sustaining alignment is a major issue in Wireless power transfer systems. Misalignment between the transmitter and receiver coils gives rise to various challenges including increasing flux leakage and decreasing mutual inductance, resulting in decreasing power transfer efficiency. A small misalignment might result in significant power losses; therefore, compensating for misalignment while maintaining high efficiency is required [5]. It is difficult to align the transmitter and receiver coils perfectly in stationary charging of electric vehicles as it relies on the driver, vehicle, and the environment. The fluctuation might be vertical, lateral, rotational, or angular. Based on the SAE J2954 standard, the wireless power transfer systems for charging electric vehicles should have the characteristic of misalignment tolerance in both horizontal and vertical directions to some extent [6]. Scholars attempt to alleviate the impact of misalignment by modifying the coil and core structure and dimension. Circular and rectangular pads were first proposed which has the advantages of simplicity in structure and required lesser winding turns which makes these structure cost-effective.

However, these topologies suffer from low coupling coefficient and less tolerance to misalignment [7],[8]. For improving misalignment performance, DD coil structure was proposed which shows a superior performance in tolerating misalignment compared to circular and rectangular structure [9]. Double D quadrature (DDQ) coupler is evolved from the DD coil structure, in which additional quadrature is added and mutually decoupled from the DD coil. DDQ coil is mostly utilized at the receiver while DD coil can be installed at the receiver or transmitter. By using the double D coil on the primary side and the DDQ coil on the secondary side, the misalignment resistance of the system enhances significantly in a way that the charging zone is three times larger than the common double D structure.[10]. The bipolar pad (BP) is suggested in order to decrease the use of copper winding and keep performance at the level of the DDQ pad [11]. The Quad D Quadrature (QDQ) coil is proposed to enhance the misalignment tolerance, which showed good toleration against misalignment for up to 50% misalignment in the lateral direction [12]. The tripolar pad topology (TPP) in the primary side is presented in [13] as a modification of the bipolar pad topology that is based on the partial overlap idea. In this setup, one transmitter pad contains three identical windings that are slightly overlapping and mutually decoupled. This topology's key benefit is that it yields a better rotational misalignment tolerance than other topologies like DD, DDQ, and BP. Integrating the compensation inductor with the main coil, which is called a dual-coupled IPT system is proposed in [14] which enhances misalignment performance. This system maintains at least 56.8% and 82.6% of the well-aligned power at 150 mm misalignment in the x and y-directions, respectively. A combined dual-coupled IPT system with a CPT system is proposed in which shows a high tolerance to misalignment in [15] which maintains at least 66.7% of well-aligned power at 200 mm.

Misalignment of the magnetic couplers causes the coupling coefficient, to deviate from the nominal value, which affects the system's efficiency, output power, input phase angle, and input impedance. Thus, it is crucial to appropriately design the compensation network to maintain efficiency as high as possible and to reduce the sensitivity to the coupling variation [16]. Four basic compensation networks such as Series-Parallel (S-P), Parallel-Series (P-S), series-series (S-S), and Parallel-Parallel (P-P), are not appropriate for working under misalignment as they are highly susceptible to misalignment [17]. LCL compensation network topology can be deployed at both the transmitter and receiver sides, which enables the transmitter side to have the constant current characteristic [18]. LCC compensation network provides higher efficiency and the primary current's amplitude is independent of mutual coupling which show high tolerance to misalignment [19]. To resolve misalignment, the authors in used a variable inductor for the primary inductor of the LCC compensation network to provide optimal switching at the inverter. To resolve misalignment, the authors in used a variable inductor for the primary inductor of the LCC

compensation network to provide optimal switching at the inverter [20]. Authors in [21] proposed an approach for tuning compensation capacitance based on receiver misalignment by using switched capacitors.

Hybrid topologies incorporate the advantages of each topology and provide a system that is resilient to changes in [22] the coupling coefficient. A combined series and LCC compensation topology is proposed in to enhance the misalignment performance. The authors in [23] proposed a simple method to optimize the resonant capacitor of a four-coil structure to improve misalignment tolerance. A particle swarm optimization with the objective function of output independent of the coupling coefficient is used in [24] for the S-CLC compensation network.

Generally, the control strategies to cope with the misalignment issue are divided into three categories: primary side control [25], secondary side control [26], and dual side control [27]. The goal of primary side control is to reduce the size and cost of the secondary side, and wireless communication is required to send data from the secondary side to the primary side for the controller. Wireless communication is prone to delay, inaccuracy which affects the operation of the controller. The primary side control can be realized by controlling the inverter or controlling the added dc-dc converter to the primary side. For controlling the switches of inverter, two parameters such duty cycle [28] and frequency [29] can be deployed to regulate the system's dynamics. Incorporation of dc-dc converter to the primary side is only required in cases when LCL or LCC compensation network is used as these topologies maintain the frequency fixed which leave the control action to other parts. The dc-dc converter is controlled to regulate the input voltage of the inverter to deal with misalignment.

The advantage of the secondary side control is that it does not require communication, which is simple and robust. However, it requires an additional circuit at the secondary side installed under the chassis of the electric vehicle, which increases the weight and cost of electric vehicles. The secondary side control to address the misalignment can be realized by controlling the rectifier [30] or controlling the additional dc-dc converter at the secondary side [31]. Dual-side control is a control scheme that controls both sides at the same time, which increases the complexity. As this control strategy controls both sides simultaneously, communication between the primary side and the secondary side is required. However, this type of control strategy is more flexible and robust. Authors in [32] Authors in [28] control the inverter and rectifier at the same time with two pulse widths, which provides high efficiency under large coupling variation due to misalignment, and has the advantage of not requiring additional dc-dc converters. Some papers applied the control scheme to the additional dc-dc converters on both sides. Scholars in [33] proposed a control strategy for controlling dc-dc converters at the primary and secondary side by estimating of coupling coefficient through load impedance variation to regulate the duty cycle of dc-dc converters to improve efficiency at misalignment conditions.

The previous research for tackling the misalignment issue is limited to a small range of misalignment while in the real world, the misalignment occurs at a higher level which most of the methods in the literature become inefficient for high misalignment and which leads to providing an autonomous alignment in some few papers. Authors in [34] used the magnetic force between transmitter and receiver to align the coil, which the transmitter coil is installed on a mechanical structure to ease self-alignment by providing a low friction path for movement. However, this system is limited to a small range of misalignment due to the limitation of the mechanical structure.

The previous research works are limited to the misalignment range, and at higher misalignment, these methods are inefficient. A self-aligning mechanism to be effective in aligning the transmitter coil to the receiver automatically in every misalignment condition, no matter how much misalignment occurs, is missing in the literature. The lack of such aligning mechanisms in the literature motivates our research group to propose a novel autonomous self-aligning system to address a wide range of misalignments in the stationary charging of electric vehicles. The autonomous self-aligning mechanism can be achieved by using a robot to align the transmitter coil to the receiver with the assistance of a magnetic field sensor to detect the magnetic field.

2. Circuit Topology

Figure 1 shows the circuit topology of the series compensated IPT system, in which a full-bridge inverter at the primary side fed the inductive coil through a compensation network. The compensation network is used to minimize reactive power to improve efficiency. The power can be transferred from the transmitter coil to the receiver coil through the magnetic field. A rectifier is used at the secondary side to convert ac to dc to supply the battery.

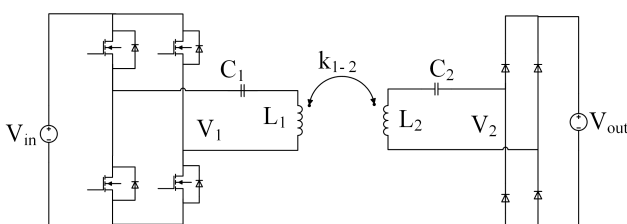


Figure 1: Circuit topology of the series compensated IPT system

3. Coil Structure

Figure 2 shows the coil structure, which is a circular pad. Ferrite bars are used at the transmitter and receiver sides to improve the coupling coefficient. Aluminum plates are used on both sides for the shielding purpose.

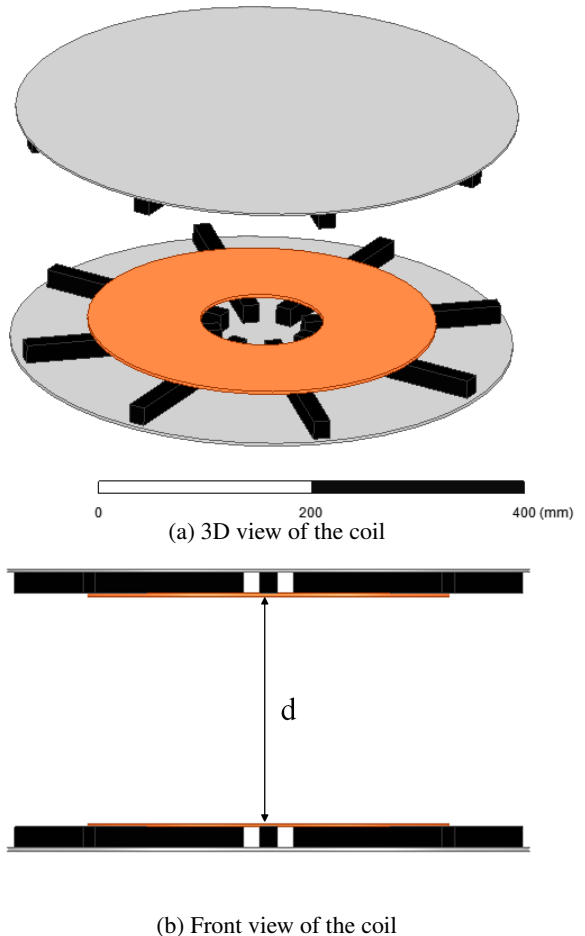


Figure 2: Structure of the coil

The magnetic field in the center of the air gap at the well-aligned can be calculated as follows:

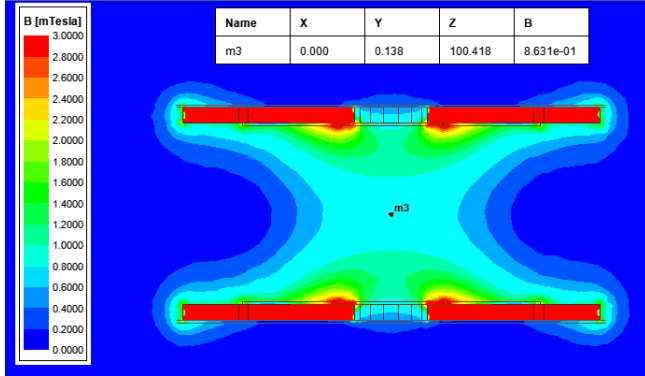
$$B = \frac{\mu_0 N I R^2}{2} \left(\frac{1}{\sqrt{(R^2 + (z - \frac{d}{2})^2)^3}} + \frac{1}{\sqrt{(R^2 + (z + \frac{d}{2})^2)^3}} \right) \quad (1)$$

where N is the number of turns, I is the current, R is the radius of the circular pad and d is the air gap. when there is misalignment in y direction as a length of d_y , the magnetic field at the center of the air gap is described as follows:

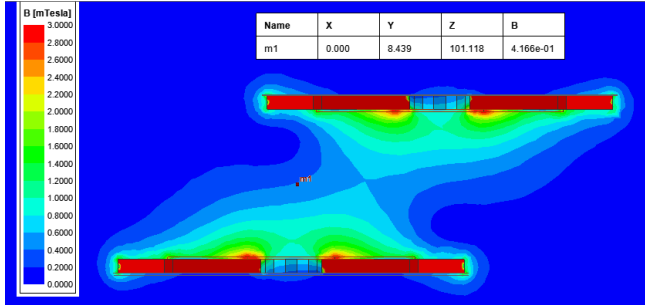
$$B = \frac{\mu_0 N I R^2}{2} \left(\frac{1}{\sqrt{(R^2 + (z - \frac{d}{2})^2)^3}} + \frac{1}{\sqrt{(R^2 + (z + \frac{\sqrt{(\frac{d}{2})^2 + d_y^2}}{2})^2)^3}} \right) \quad (2)$$

According to eq. 2, the magnetic field strength in the midpoint between transmitter and receiver is decreased by increasing misalignment (d_y).

Figure 3 demonstrates the magnetic field distribution in the well-aligned case and when the transmitter and receiver have 20cm misalignment. As shown in Figure 3, when the transmitter coil is well-aligned with receiver coil, the magnetic field strength at the midpoint between the transmitter and receiver is 0.8 mT. While at the 20 cm misalignment, the magnetic field strength at the mid-point between the transmitter and receiver is half of the magnetic field value in a well-aligned case. This proves that the misalignment gives rise to a reduction in magnetic field strength at the air gap between the transmitter and receiver coils.



(a) Magnetic field distribution at well-aligned



(b) Magnetic field distribution at 20cm misalignment

Figure 3: Magnetic field distribution

Figure 4 shows the coupling coefficient between the transmitter and receiver in different misalignments. As shown in Figure 4, the misalignment gives rise to a significant reduction in the coupling coefficient, in which at 25cm misalignment, the coupling coefficient reaches zero.

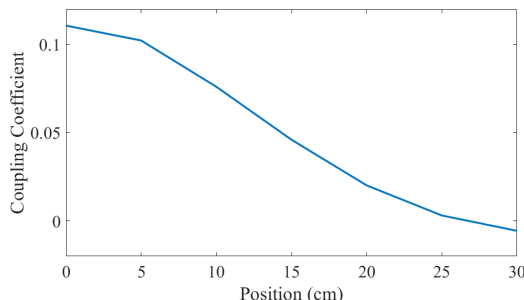


Figure 4: Coupling coefficient between transmitter and receiver at different misalignment

4. Proposed Autonomous Alignment system

To improve the misalignment performance, an autonomous alignment system is proposed, in which the transmitter pad is mounted on a robot to move. A magnetic field sensor is installed on the transmitter pad, which follows the highest magnetic field. The highest magnetic field is in the well-aligned case, which the transmitter and receiver are well-aligned. In this case, by having misalignment, the transmitter pad moves to remove misalignment and create alignment. In other words, the transmitter follows the receiver to remove misalignment. Fig. 1 shows the structure of the proposed system. As shown in Fig. 1, the transmitter coil is mounted on a robot to move the transmitter. A magnetic field sensor is installed on the transmitter pad to measure the magnetic field. The measured magnetic field is compared with the highest magnetic field value, and the error sends to the controller. The controller sends a command to the robot to move the transmitter to reduce the error to align with the transmitter.

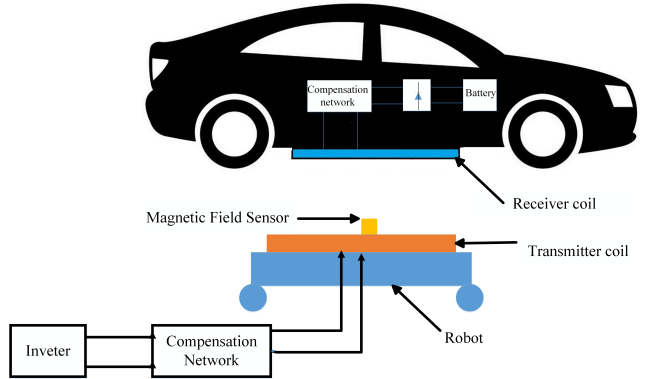


Figure 5: The structure of the proposed autonomous alignment system

4.1. Design process of the robot's structure

The robot should be designed properly, so that can tolerate the weight of the transmitter coil without affecting the speed and movement of the robot. In this section, the design process of the robot is discussed in detail. The Chassis is made of a Galvanized Steel Frame that goes around in an octagonal shape. This frame is strong enough to support the transmitter coil and is a solid foundation for all the other parts that would be implemented. Figure 6 shows the structure of the Galvanized steel frame.

The frame then is supported additionally by another bar in the middle that will contribute to better stability and strength. This steel bar will also hold the motors. The motors are off-brand 12V motors that have high torque. Because of the torque, it can handle a large sum of weight. With the 4-inch size of the wheels on the motors, the total platform can haul a little over 35 pounds. The downside of this type of motor is that it is not very fast, but it is still able to push the required amount of weight. Figure 7 shows the steel bars hold the motors.



Figure 6: Galvanized steel frame



Figure 7: Steel bar that also holds the motors

This frame will support a PVC platform. This platform will hold the transmitter coil and the magnetic field sensor. Underneath this platform, another PVC platform was created to house future components such as battery packs and microcontrollers. The frame was supported by two wheels powered by 12V motors and 4 Caster Wheels. The caster wheels give the flexibility to move, and allow for good stability while providing a firm foundation. Figure 8 shows the caster wheels used to support the frame.

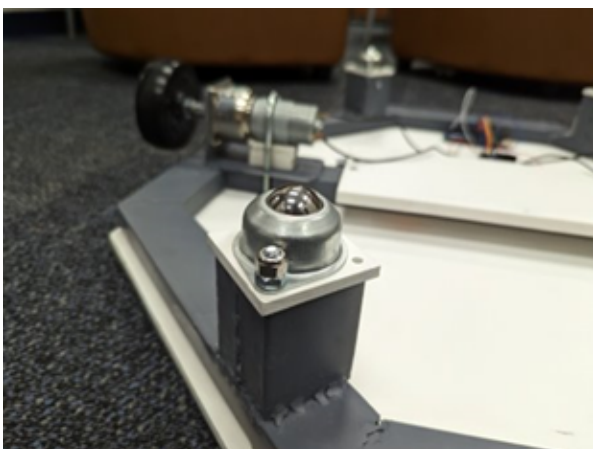


Figure 8: Caster wheels used to support the frame

All these components came together to get the current version of the alignment system's chassis. This chassis is very strong and durable. It has the space and strength to hold the transmitter coil and all the future components. The overall chassis weighs around 30 pounds with the transmitter coil. Figure 9 shows the complete chassis for holding the transmitter coil.

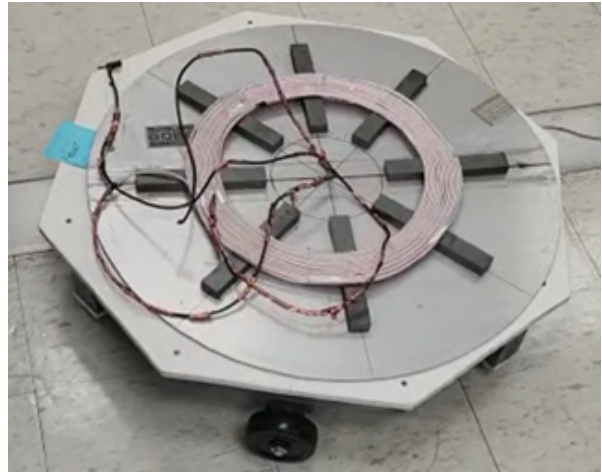


Figure 9: Completed chassis for holding transmitter coil

4.2. The control mechanism of the self-aligning system

Figure 10 shows the block diagram of the proposed autonomous self-aligning. The entire system takes in two inputs and has one output. An existing magnetic field will be taken as an input to the magnetic field strength detection unit. The transmitter coil within the detection unit will use its own power supply to contribute to the strength of the existing magnetic field. The microcontroller receives magnetic field strength values from the hall effects sensor, which it then uses to perform calculations and logic on those values and outputs motor instructions. Since the motors cannot understand these instructions, the motor shield serves as the interface that translates these instructions for the motors to adjust the chassis position accordingly.

This section focuses on a highly specialized algorithm that is specifically designed to control the EV Wireless Charging Alignment System. This algorithm is critical in aligning the transmitter coil to the receiver coil to maximize their power transfer. This algorithm's unique and complex nature demands exceptional attention and understanding to ensure the effective functioning of the charging device. This section will delve deeply into the inner workings of this algorithm and explore its intricacies and nuances to gain a comprehensive understanding of its capabilities and limitations. It will explain the algorithm in detail, including its functionality, applications, and notable characteristics. By providing an in-depth analysis of this algorithm, this section aims to provide a comprehensive understanding of its workings, potential, and limitations and to highlight its

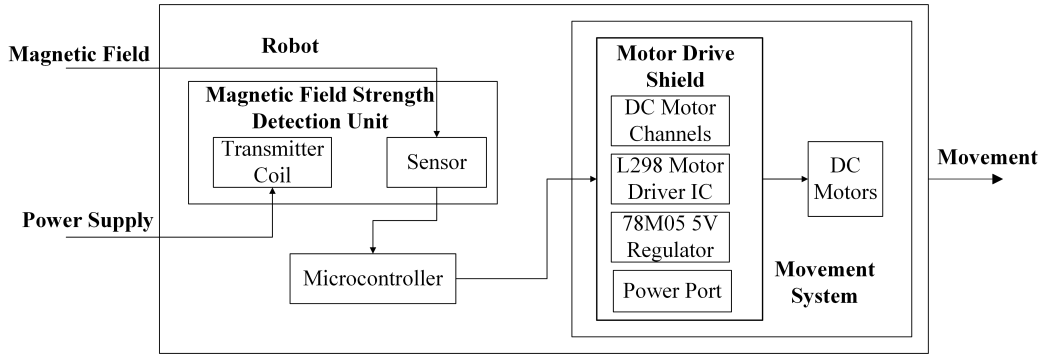


Figure 10: Block diagram of the proposed autonomous self-aligning system

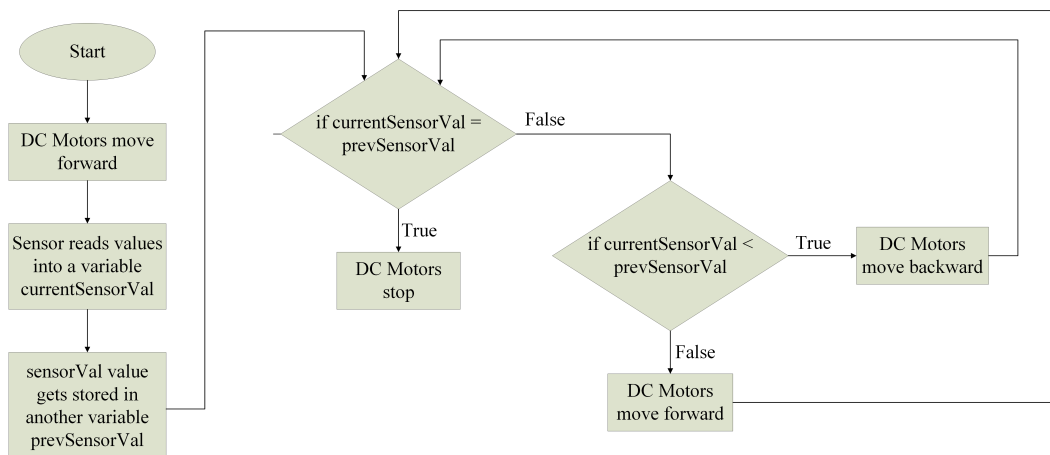


Figure 11: Flowchart of the forward single-axis algorithm

importance in the field of electric vehicle wireless charging and its potential to revolutionize the industry.

This section also explains the algorithm that was fully developed and tested. The concept for this algorithm was designed to be as straightforward as possible to follow a test-driven development (TDD) and Agile approach, even though no test harnesses were used in conglomeration with the Arduino integrated development environment (IDE). This simplicity has several advantages with respect to the goal and expectations of this product as well as the current development stage. The following are some general goals and expectations for the project that drove the decision to take a simplistic approach and were taken into consideration when developing the algorithms.

There are three possible algorithms for realizing autonomous self-aligning mechanism which are as follows:

1- Forward Single-Axis: The algorithm that is currently used and tested in the laboratory setting. This algorithm, when powered on, tells the motors to move forward. The alignment system will then move forward until a hardcoded setpoint value is received from the sensor. When the microcontroller gets the setpoint value from the sensor, it will tell the motors to stop. This only goes in one access. 2- Double Single-Axis Alignment: This algorithm was developed but was not able to be tested in the laboratory setting. This

algorithm will tell the alignment system to move forward until the hardcoded setpoint value is received. After that value is received, it will turn 90 degrees and move to the second axis and stop after it determines the highest set-point value.

3- Spiral: This algorithm was developed but was not able to be tested in the laboratory setting. This algorithm will move forward until the setpoint value is reached. Afterward, the system will move in a shape like a spiral and gauge all the values in the area and stop at the highest one.

The forward single-axis algorithm is tested and implemented in this paper. Figure 11 shows the flowchart of the forward single-axis algorithm.

Figure 14 shows the implemented proposed algorithm in the real world. As shown in Figure 14, Onto the chassis, two 12V motors were fitted onto the sides to propel the chassis in the desired direction. These motors were connected to the 3A L298N motor shield. This motor shield is strong enough to support the combined 24V battery pack giving to the motors. The motor shield also allows for better controllability of the individual motors by providing individual settings for the direction and speed of each motor. This motor shield takes power from the power banks and powers the motor.

The motor shield gets instructions from the Arduino Mega 2560 Microcontroller to move the motors according to

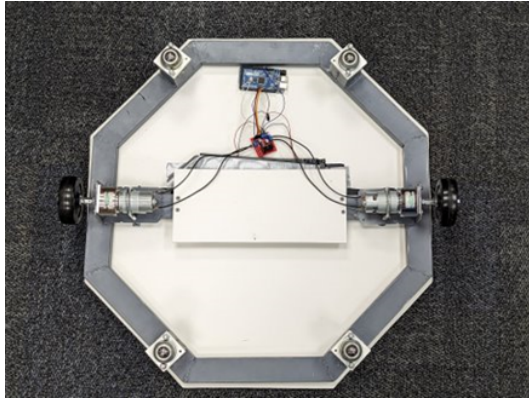


Figure 12: Implemented proposed algorithm in the real world

the implemented algorithm. The Mega is more than capable of executing the instructions that we give to it. Since it is a larger controller, it has the space to accommodate for additional features that could be implemented in the future such as more sensors. Figure 15 shows the motor shield and hidden power bank.

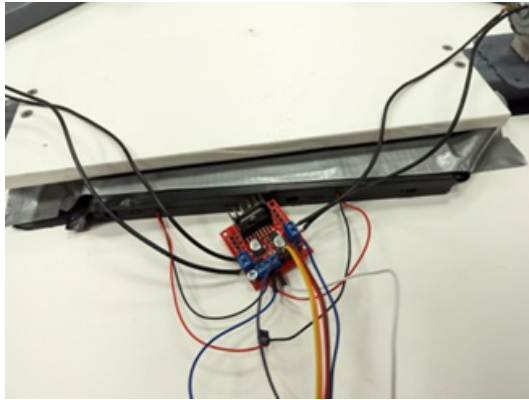


Figure 13: Motor shield and hidden power bank

The Arduino Mega 2560 Microcontroller processes logic based on the sensor values that are obtained through the hall effect sensor that is attached to the top of the alignment system. The Hall effect sensor is able to read the values from the magnetic field that the coils produce and accurately gives those values to the Arduino Mega 2560 to use. The proposed algorithm also has the ability to calculate the percentage of misalignment between the transmitter and receiver coil. The magnetic field value at well-aligned is used as a reference and compared with measured different values as the transmitter coil approached the receiver coil. The calculation was based on the following equation to display the misalignment:

$$Misalignment\% = \frac{B_{measured} - B_{ref}}{B_{ref}} * 100 \quad (3)$$

where:

$B_{measured}$: magnetic field value read by sensor
 B_{ref} : The magnetic field value at well-aligned

Table 1
Coupler's Dimension and Circuit Specification

Parameter	Value	Parameter	Value
V_{in}	25 V	V_{out}	25 V
coil's internal dia	117mm	Width of the coil	107mm
Ferrite bar length	192mm	Ferrite bar width	18mm
Shielding plate dia	750mm	Number of turns	15
L_1, L_2	$172\mu H$	C_1, C_2	120nF
air gap (d)	200mm	f	35 kHz

5. Experimental Results

After designing the coupler, the circuit parameters are tuned for realizing resonance at the frequency of 35 kHz. Table 1 shows the coupler's dimensions and circuit specifications.

Using the parameters in Table 1, a prototype of the system is constructed which is shown in Figure 14.



Figure 14: Experimental prototype of the system

The transmitter and receiver coil are composed of AWG 36 Litz wire to minimize skin effect losses. For the implementation of the input inverter, silicon-carbide (SiC) MOSFETs C2M0025120D are utilized to minimize conduction losses. Texas Instruments TMS320F28379D digital microcontroller is used for the generation of the MOSFETs PWM signals. The digital microcontroller has the advantage of being convenient in adjusting the frequency and dead time for the full-bridge inverter. In this paper, the dead time is selected to be 100ns. Figure 12 shows the output voltage of the inductive power transfer.

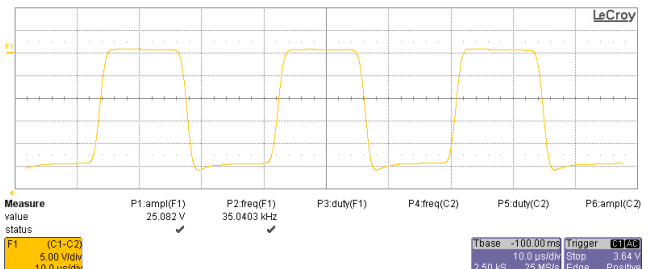


Figure 15: Output voltage of inductive power transfer

To test the effectiveness of the proposed autonomous self-aligning mechanism, the receiver is placed with 30 cm misalignment with respect to the transmitter coil mounted

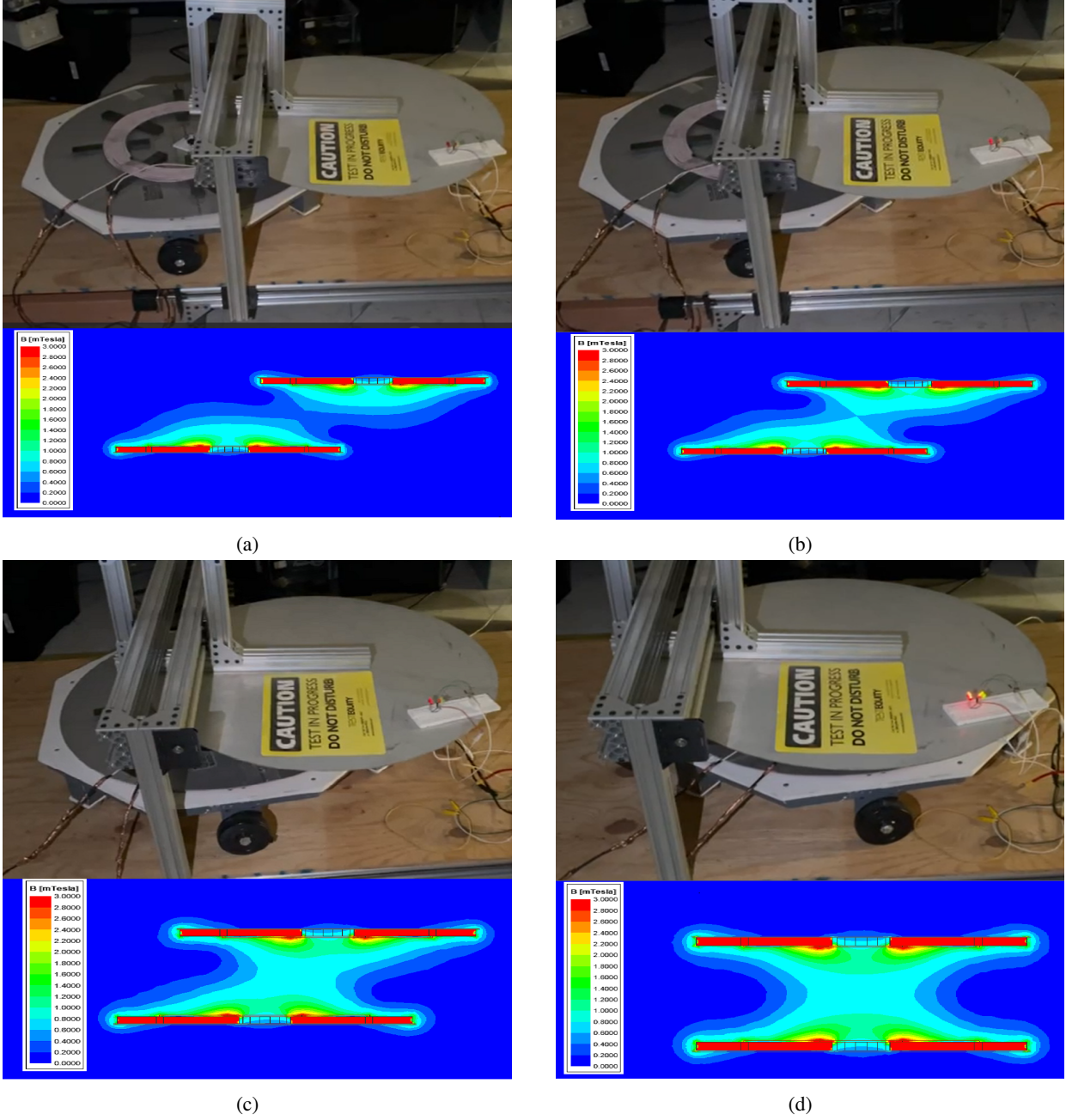


Figure 16: Experimental results: a) 30cm misalignment; b) 20cm misalignment; c) 10cm misalignment; and, d) well-aligned

on the robot. The magnetic field sensor at the center of the transmitter's coil reads the magnetic field value, and by using the proposed algorithm, the robot moves forward to find the magnetic field value at the well-aligned. When the transmitter's coil mounted on the robot reach the alignment point, the robot is stopped. The alignment is created automatically and without human interference. Figure 16 shows the experimental results of the autonomous self-aligning mechanism as the transmitter's coil on the robot automatically follows the receiver to make the alignment. A video of the robot's movement toward the receiver is created, but it is not possible to provide a video in the PDF. Due to this reason, a snapshot of 4 different misalignment cases is

provided with the respective magnetic field distribution in Figure 16. Five LEDs are connected in series at the output side of the inductive power transfer to show whether the power is transferred or not in different misalignment cases. It is worth mentioning as these five LEDs are connected in series; therefore, 25V is required to turn the LEDs on. As shown in Figure 16(a) the receiver is placed with 30 cm misalignment, which the power can not be transferred, as the LEDs are off. The robot starts traveling toward the receiver, and the snapshot of its movement at 20 cm misalignment is provided in Figure 16 (b). As no alignment is created, the robot moves further, and its snapshot at 10cm misalignment is shown in Figure 16 (c). Since a partial alignment is created

at 10cm misalignment, some of the LEDs are turned on. The robot moves further, and as the full alignment happened, the robot is stopped and all LED's turned on, which is shown in Figure 16 (d).

6. Conclusion and Future Works

An autonomous self-aligning mechanism for addressing misalignment issues in the stationary charging of electric vehicles is proposed. The proposed mechanism uses a robot to move the transmitter to follow the receiver pad based on measuring the magnetic field. The design process of the robot by considering the transmitter's coil weight and the required torque for the dc motors to move the transmitter's coil is discussed in detail. Three algorithms are proposed for self-aligning the transmitter coil to the receiver coil, and the forward self-aligned algorithm is implemented in the laboratory. The experimental results validate the effectiveness of the proposed autonomous self-aligning mechanism in making alignment between the transmitter's coil and receiver coil. The future work lines into implementing a double single-axis algorithm in the laboratory, which addresses the horizontal and vertical misalignment problem.

7. Acknowledgment

The authors acknowledge the support provided by the senior design team (Christopher Prasad, Maximiliano Mauna, Andy Alvarez, Rodolfo Ramos, and Ivan Mendoza) in theory and experimental work.

References

- [1] Siqi Li and Chunting Chris Mi. "Wireless power transfer for electric vehicle applications". In: *IEEE journal of emerging and selected topics in power electronics* 3.1 (2014), pp. 4–17.
- [2] Fei Lu, Hua Zhang, and Chris Mi. "A review on the recent development of capacitive wireless power transfer technology". In: *Energies* 10.11 (2017), p. 1752.
- [3] Milad Behnamfar, Hamid Javadi, and Ebrahim Afjei. "A dynamic CPT system LC Compensated with a six-plate capacitive coupler for wireless charging of electric vehicle in motion". In: *2020 28th Iranian Conference on Electrical Engineering (ICEE)*. IEEE. 2020, pp. 1–6.
- [4] Changsong Cai et al. "A cost-effective segmented dynamic wireless charging system with stable efficiency and output power". In: *IEEE Transactions on Power Electronics* 37.7 (2022), pp. 8682–8700.
- [5] Xian Zhang et al. "Influence of misalignment of electric vehicle wireless charging system coupling structure on magnetic field distribution". In: *2018 IEEE 2nd International Electrical and Energy Conference (CIEEC)*. IEEE. 2018, pp. 553–556.
- [6] Zhicong Huang, Siu-Chung Wong, and K Tse Chi. "Control design for optimizing efficiency in inductive power transfer systems". In: *IEEE Transactions on Power Electronics* 33.5 (2017), pp. 4523–4534.
- [7] Mickel Budhia, Grant A Covic, and John T Boys. "Design and optimization of circular magnetic structures for lumped inductive power transfer systems". In: *IEEE Transactions on Power Electronics* 26.11 (2011), pp. 3096–3108.
- [8] Roman Bosshard et al. "Modeling and $\eta - \alpha$ -Pareto Optimization of Inductive Power Transfer Coils for Electric Vehicles". In: *IEEE Journal of Emerging and Selected Topics in Power Electronics* 3.1 (2014), pp. 50–64.
- [9] Kai Song et al. "Design of DD coil with high misalignment tolerance and low EMF emissions for wireless electric vehicle charging systems". In: *IEEE Transactions on Power Electronics* 35.9 (2020), pp. 9034–9045.
- [10] Mickel Budhia et al. "Development of a single-sided flux magnetic coupler for electric vehicle IPT charging systems". In: *IEEE Transactions on Industrial Electronics* 60.1 (2011), pp. 318–328.
- [11] Adeel Zaheer, Grant A Covic, and Dariusz Kacprzak. "A bipolar pad in a 10-kHz 300-W distributed IPT system for AGV applications". In: *IEEE Transactions on Industrial Electronics* 61.7 (2013), pp. 3288–3301.
- [12] Kafeel Ahmed et al. "A new coil design for enhancement in misalignment tolerance of Wireless Charging System". In: *2015 IEEE Student Conference on Research and Development (SCoReD)*. IEEE. 2015, pp. 215–219.
- [13] Seho Kim, Grant A Covic, and John T Boys. "Comparison of tripolar and circular pads for IPT charging systems". In: *IEEE Transactions on Power Electronics* 33.7 (2017), pp. 6093–6103.
- [14] Fei Lu et al. "A dual-coupled LCC-compensated IPT system with a compact magnetic coupler". In: *IEEE Transactions on Power Electronics* 33.7 (2017), pp. 6391–6402.
- [15] Milad Behnamfar, Hassan Jafari, and Arif Sarwat. "Development of a Mixed Inductive and Capacitive Wireless Power Transfer to Improve Misalignment Performance for Charging Electric Vehicles". In: *2022 IEEE Transportation Electrification Conference & Expo (ITEC)*. IEEE. 2022, pp. 600–605.
- [16] Ali Ramezani and Mehdi Narimani. "Optimized electric vehicle wireless chargers with reduced output voltage sensitivity to misalignment". In: *IEEE Journal of Emerging and Selected Topics in Power Electronics* 8.4 (2019), pp. 3569–3581.
- [17] Devendra Patil et al. "Wireless power transfer for vehicular applications: Overview and challenges". In: *IEEE Transactions on Transportation Electrification* 4.1 (2017), pp. 3–37.
- [18] Udaya K Madawala and Duleepa J Thrimawithana. "A bidirectional inductive power interface for electric vehicles in V2G systems". In: *IEEE Transactions on Industrial Electronics* 58.10 (2011), pp. 4789–4796.
- [19] Weihan Li et al. "Integrated LCC compensation topology for wireless charger in electric and plug-in electric vehicles". In: *IEEE Transactions on Industrial Electronics* 62.7 (2014), pp. 4215–4225.
- [20] Samer Aldhaher et al. "Wireless power transfer using Class E inverter with saturable DC-feed inductor". In: *IEEE Transactions on Industry Applications* 50.4 (2014), pp. 2710–2718.
- [21] Kimberley A Cota et al. "An approach for selecting compensation capacitances in resonance-based EV wireless power transfer systems with switched capacitors". In: *IEEE Transactions on Transportation Electrification* 5.4 (2019), pp. 1004–1014.
- [22] Lei Zhao, Duleepa J Thrimawithana, and Udaya K Madawala. "Hybrid bidirectional wireless EV charging system tolerant to pad misalignment". In: *IEEE Transactions on Industrial Electronics* 64.9 (2017), pp. 7079–7086.
- [23] Qingwei Zhu et al. "Improving the misalignment tolerance of wireless charging system by optimizing the compensate capacitor". In: *IEEE Transactions on Industrial Electronics* 62.8 (2015), pp. 4832–4836.
- [24] Yousu Yao et al. "Particle swarm optimization-based parameter design method for S/CLC-compensated IPT systems featuring high tolerance to misalignment and load variation". In: *IEEE Transactions on Power Electronics* 34.6 (2018), pp. 5268–5282.

- [25] Farzad Farajizadeh et al. “Expandable N-legged converter to drive closely spaced multitransmitter wireless power transfer systems for dynamic charging”. In: *IEEE Transactions on Power Electronics* 35.4 (2019), pp. 3794–3806.
- [26] Jia Liu, Zhitao Liu, and Hongye Su. “Passivity-based PI control for receiver side of dynamic wireless charging system in electric vehicles”. In: *IEEE Transactions on Industrial Electronics* 69.1 (2021), pp. 783–794.
- [27] Minkook Kim, Dong-Myoung Joo, and Byoung Kuk Lee. “Design and control of inductive power transfer system for electric vehicles considering wide variation of output voltage and coupling coefficient”. In: *IEEE Transactions on Power Electronics* 34.2 (2018), pp. 1197–1208.
- [28] José Manuel González-González, Alicia Triviño-Cabrera, and José Antonio Aguado. “Design and validation of a control algorithm for a SAE J2954-compliant wireless charger to guarantee the operational electrical constraints”. In: *Energies* 11.3 (2018), p. 604.
- [29] Eleni Gati, Georgios Kampitsis, and Stefanos Manias. “Variable frequency controller for inductive power transfer in dynamic conditions”. In: *IEEE Transactions on power electronics* 32.2 (2016), pp. 1684–1696.
- [30] Kerim Colak et al. “A novel phase-shift control of semibridgeless active rectifier for wireless power transfer”. In: *IEEE Transactions on Power Electronics* 30.11 (2015), pp. 6288–6297.
- [31] WX Zhong and SYR Hui. “Maximum energy efficiency tracking for wireless power transfer systems”. In: *IEEE Transactions on Power Electronics* 30.7 (2014), pp. 4025–4034.
- [32] Tobias Diekhans and Rik W De Doncker. “A dual-side controlled inductive power transfer system optimized for large coupling factor variations and partial load”. In: *IEEE Transactions on Power Electronics* 30.11 (2015), pp. 6320–6328.
- [33] Xin Dai et al. “Maximum efficiency tracking for wireless power transfer systems with dynamic coupling coefficient estimation”. In: *IEEE Transactions on Power Electronics* 33.6 (2017), pp. 5005–5015.
- [34] Alireza Namadmalan et al. “Self-Aligning Capability of IPT Pads for High-Power Wireless EV Charging Stations”. In: *IEEE Transactions on Industry Applications* 58.5 (2022), pp. 5593–5601.